Particulate matter air quality assessment using integrated surface, satellite, and meteorological products: Multiple regression approach

Pawan Gupta[1] and Sundar A. Christopher[1]

Received 20 November 2008; revised 29 April 2009; accepted 7 May 2009; published 28 July 2009.

[1] Monitoring particulate matter air quality from spaceborne measurements is largely confined to relating columnar satellite retrievals of aerosol optical thickness (AOT) with ground measurements of PM2.5 mass concentration. However, vertical distribution of aerosols and meteorological effects such as wind speed, temperature, and humidity also play a major role in this AOT-PM2.5 relationship. In this study, using 3 years of coincident hourly PM2.5 mass concentration (PM2.5 or $PM_{2.5}$), Moderate Resolution Imaging Spectroradiometer–derived AOT, and rapid update cycle meteorological fields, we developed multiple regression equations as function of season for 85 P.M2.5 monitors over the southeastern United States. Our goal is to examine whether the use of meteorological fields will improve the relationship between PM2.5 and AOT. Our results indicate that there is up to threefold improvement in the correlation coefficients while using meteorological information through multiple regression methods compared to two variant regression (AOT versus PM2.5) equations. A 20–50% improvement in root-mean-square error is observed when adding temperature and boundary layer height to the AOT-PM2.5 relationship. The best agreement between AOT and PM2.5 was found during summer and in well-mixed boundary layer regimes. Since boundary layer heights are readily available from model simulations over the United States, they can be used as a good surrogate for estimating aerosol heights in conjunction with space- and ground-based lidars. These results and analysis are useful to research and operational communities that seek to improve the use of satellite information for assessing surface PM2.5.

Citation: Gupta, P., and S. A. Christopher (2009), Particulate matter air quality assessment using integrated surface, satellite, and meteorological products: Multiple regression approach, *J. Geophys. Res.*, *114*, D14205, doi:10.1029/2008JD011496.

1. Introduction

[2] Particulate matter with aerodynamic diameters less than 2.5 μm (PM2.5 or $PM_{2.5}$) can cause respiratory and lung diseases and even premature death [*Krewski et al.*, 2000]. Using statistical data collected in 20 big cities, *Samet et al.* [2000] showed that the daily mortality within a metropolitan area is associated with concurrent or lagged daily fluctuations in ambient PM concentrations. Poor air quality conditions are also associated with damaging buildings and monuments around the world. Indirectly, air pollution significantly affects the economy by increasing medical expenditures and for preserving the surrounding environment.

[3] Several research papers have outlined the methods by which different satellite products can be used to obtain surface PM2.5 [e.g., *Wang and Christopher*, 2003; *Engel-Cox et al.*, 2006; *Hutchison et al.*, 2005; *Gupta et al.*, 2006; *Liu et al.*, 2004; *van Donkelaar et al.*, 2006]. In summary, first the columnar satellite-derived aerosol optical thickness (AOT) at 0.55 μm values are related to surface PM2.5 mass measurements. Then a linear regression equation is used to convert the satellite AOT measurements to PM2.5 mass concentration and then to air quality indices based on EPA guidelines [e.g., *Al-Saadi et al.*, 2005]. It is important to note that AOT is an unit less optical representation of the column loading of atmospheric aerosols whereas PM2.5 is mass concentration of particles less than 2.5 μm in aerodynamic diameter measured at surface in units of μgm^{-3}. Satellite measured AOT can empirically be converted into PM2.5 mass by knowing aerosol microphysical and optical properties along with height of aerosol layer in the atmosphere. The details on this type of conversion can be found else where [i.e., *Koelemeijer et al.*, 2006]. However, most studies have concluded that the PM2.5-AOT relationship alone cannot be used to estimate surface level PM2.5 since the vertical distribution of aerosols and other meteorological parameters such as humidity and temperature could also be important [*Liu et al.*, 2005; *Paciorek et al.*, 2008]. Since the satellite measurements provide columnar retrievals, relating this to surface values requires information about the vertical distribution of aerosols. If aerosols are transported aloft and the satellite retrievals have reported values for AOT, this does not necessarily mean that the ground monitors capture that event. In this case relating the AOT to PM2.5 values is not meaningful.

[1]Department of Atmospheric Sciences, University of Alabama in Huntsville, Huntsville, Alabama, USA.

0148-0227/09/2008JD011496

[4] The vertical distribution of aerosols can be inferred from ground-based [*Fernald*, 1984; *Ansmann et al.*, 2000] and from spaceborne LIDARs such as CALIPSO [*Winker et al.*, 2003]. Radar and satellite data could also be useful for estimating heights of aerosol layers [*Melnikov et al.*, 2008]. However, there are various limitations with some of these data sets. The swath width of spaceborne lidars such as CALIPSO is very narrow and global coverage is only achieved over several weeks. Ground-based lidars on the other hand are sparse in spatial coverage and do not operate on a continual basis. Using limited observations of vertical distribution of aerosols from lidars, some studies have demonstrated that aerosols are well mixed and mostly confined within the planetary boundary layer (PBL) [*Ansmann et al.*, 2000]. Thus, the height of PBL (HPBL) or the day time mixing layer height can be used as a good surrogate to estimate the height of the aerosol layer. The HPBL can be used to scale the column AOT value into boundary layer extinction value [*Liu et al.*, 2005] to improve the AOT-PM2.5 linear regression relationships. Other parameters such as humidity could also affect this AOT-PM2.5 relationship owing to hygroscopic growth of aerosols. Therefore, in this paper we assess whether the use of meteorological parameters will improve the relationship between AOT and PM2.5. We construct simple AOT-PM2.5 relationship that we call two-variate method (TVM) and then compare this to a multivariate method (MVM) that utilizes various meteorological parameters.

2. AOT-PM2.5 Assessment Using Meteorology

[5] Fine particular matter in the atmosphere is produced by gas to particle conversion mechanism as well as through various sources due to anthropogenic and natural activities. The meteorological conditions that strongly influence the concentration of PM2.5 particles include temperature, relative humidity and height of planetary boundary layer [*Seinfeld and Pandis*, 2006]. Other processes that impact PM2.5 concentration include small- to large-scale transport by winds, horizontal and vertical dispersion, variations in available sunlight for photochemical reactions due to clouds and seasons, temperature gradients, available moisture, and most importantly the dilution of pollution in atmospheric boundary layer due to changes in vertical mixing. The variability in these meteorological conditions is primarily governed by large-scale high and low pressure systems, diurnal heating and cooling, and topography. Temperature can enhance the photochemical reactions in the atmosphere and hence production of PM2.5 particles. Temperature inversion can also reduce the vertical mixing and therefore increase chemical concentration of precursors. Higher concentration of precursors produces faster and more efficient chemical processes that convert gaseous emissions into particles. High relative humidity can enhance the growth and production of secondary particles and hence change the size distribution of particles as well as change in optical properties by modifying scattering efficiencies [*Wang and Martin*, 2007].

[6] Dilution of pollution due to change in HPBL and moisture content are of significant importance in satellite remote sensing of particulate matter. PM2.5 mass concentrations measured at the surface will be low during conditions of high HPBL compared to conditions of low boundary layer heights whereas satellite will measure almost the same columnar AOT. Figure 1 presents a schematic of two different cases of temperature inversion, HPBL, and their influence on surface measured PM2.5 mass concentration. In the first case (Figure 1, top), vertical temperature profiles show weak and high inversion, which are easily broken down owing to solar heating at sunrise while the boundary layer starts growing and reaches to a maximum height during the afternoon hours. As a result of increase in HPBL, existing pollution levels are diluted in the growing boundary layer and hence surface-based instruments will measure reduced PM2.5 mass concentration values. In the second case (Figure 1, bottom), strong and low inversion does not allow growth of HPBL owing to solar heating, therefore slowing down the process of dilution. In this case the surface stations measure high PM2.5 mass concentrations when compared to the first case. These are some common scenarios, but sometimes if nocturnal inversion is strong and solar heating is weak, the inversion may not break until late in the day or at all. These conditions produce high concentrations of pollution near the surface owing to lack of vertical mixing. Surface and column measurement during such days may not relate very well to each other. In all cases, spaceborne measurements will still measure columnar loading of the aerosols and hence theoretically the AOT should remain constant. Therefore, accounting for proper HPBL in estimation of PM2.5 is important when using satellite-retrieved AOT.

3. Data and Study Area

[7] To assess surface level PM2.5, 3 years of (2004–2006) hourly PM2.5 mass concentrations from the ground stations, Terra-Moderate Resolution Imaging Spectroradiometer (MODIS) AOT at 0.55μm and meteorological fields from hourly rapid update cycle (RUC) reanalysis over 85 AirNow stations in southeast United States are used (Figure 2). Table 1 provides details on the different data sets and sections 3.1–3.3 describe each data set in more detail.

3.1. Surface PM2.5 Mass

[8] The U.S. Environmental Protection Agency (EPA) and its state partners maintain several air quality monitoring networks in the United States. These networks monitor the mass concentration of particulate air pollutants at the ground. PM2.5 data from these networks include 24-h average (daily) and hourly PM2.5 mass concentrations. The PM2.5 mass measured in μgm^{-3} is most relevant to the present study. This study uses both hourly and daily mean PM2.5 mass concentration data sets from 85 ground stations as shown in Figure 2. $PM_{2.5}$ mass concentration over these stations is measured using a Tapered-Element Oscillating Microbalance (TEOM) instrument with an accuracy of ±1.5 μgm^{-3} for hourly averages although it may underestimate PM2.5 mass concentration owing to volatilization of ammonium nitrate and organic carbon [*Grover et al.*, 2005]. Hourly average PM2.5 mass concentration values are used to derive air quality categories whereas daily mean values are used to monitor and assess the air quality. Air quality categories represent ranges of air quality index that are used

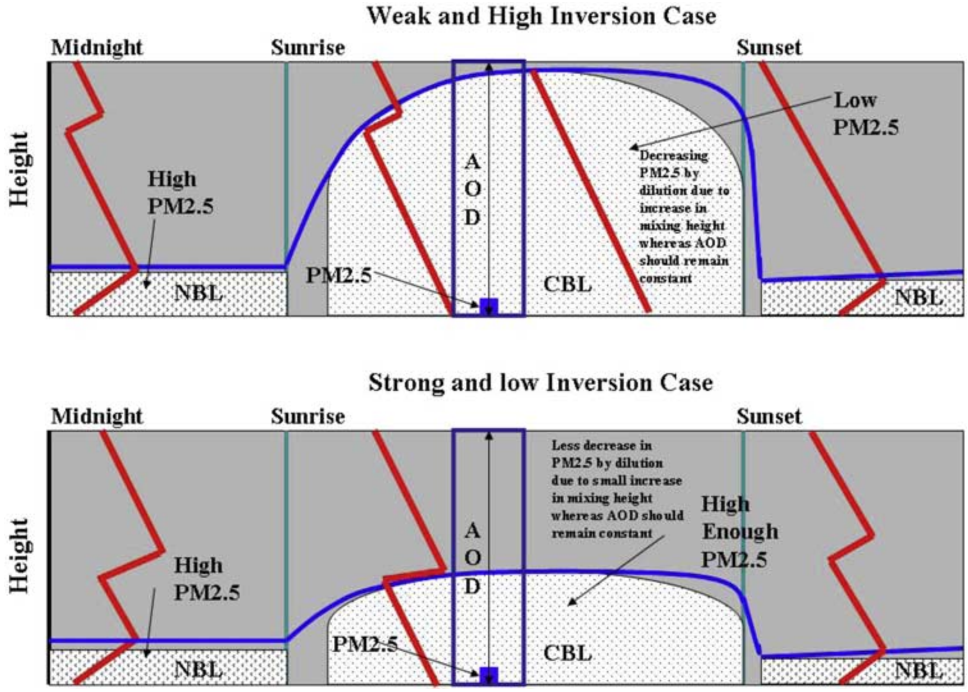

Figure 1. Schematic showing evaluation and growth of planetary boundary layer height under weak and strong temperature inversion conditions.

by USEPA to establish a relationship between mass concentration and human health.

3.2. Satellite Aerosol Data

[9] The MODIS instruments onboard NASA's Terra (equatorial crossing time of 1030 LT) and Aqua (equatorial crossing time of 1330 LT) satellites provide routine retrievals of cloud and aerosol properties over land [*Remer et al.*, 2005]. MODIS provides spectral information of aerosol optical properties in seven different wavelengths over ocean and in three wavelengths over land [*Levy et al.*, 2007]. The AOT, representing the columnar loading of aerosols in the atmosphere, is an important aerosol parameter retrieved from satellite observations. Recently, a

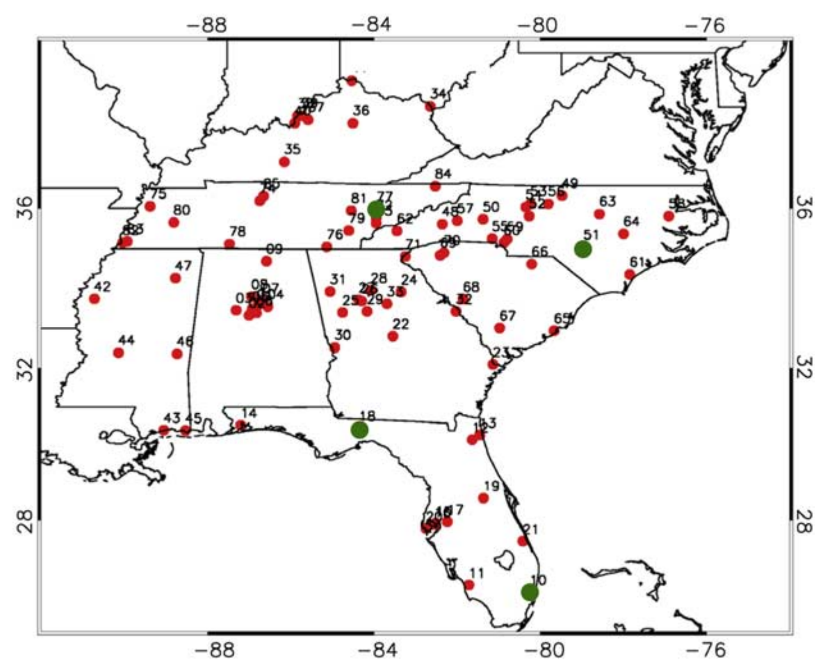

Figure 2. Study area showing major cities in the area along with locations of PM2.5 monitoring stations under the EPA AirNow network.

Table 1. Detailed Information on Various Surface, Model, and Satellite Data Sets Used for Particulate Matter Air Quality Assessment in the Southeast United States

	Parameters	Sensors	Temporal Resolution	Resolution	Source
1	PM2.5	TEOM	Hourly	Point measurements	EPA's AirNow-Tech
2	AOT, CF	MODIS-Terra Satellite (MOD04)	Instantaneous	10 × 10 km	Level 1 and Atmosphere Archive and Distribution System (LAADS) at Goddard Space Flight Center
3	Meteorological fields	RUC reanalysis	Hourly	20 × 20 km	Atmospheric Radiation Measurement (ARM) data archive

new version of the MODIS algorithm (collection 5, V5.2) has replaced an older version (collection 4, V5.1). The new algorithm uses new aerosol models and improved estimation of surface reflectance. This algorithm applies stringent criteria to select appropriate pixels in the retrieval process thereby reducing the total number of data points [*Levy et al.*, 2007]. Several validation studies over AERONET locations conducted over global land reveal that 57% of MODIS AOT retrievals (collection 4) are within expected uncertainty levels of $\pm 0.05 \pm 0.15$*AOT [*Remer et al.*, 2005]. Preliminary results from a validation exercise of MODIS collection 5 shows that 72% of the retrievals fall within that expected uncertainty over land [*Remer et al.*, 2008], which is an improvement over the previous collection 4 data sets. MODIS aerosol product also provides the fractional cloud cover for each pixel and it is obtained during cloud masking process in the aerosol retrieval algorithm. More details on the algorithm can be found in the work by *Levy et al.* [2007].

3.3. Meteorology from RUC Analysis

[10] The rapid update cycle (RUC or RUC20 with 20 km grid resolution) is an operational atmospheric prediction and assimilation system composed of a numerical forecast model and an analysis system to initialize that model. The RUC has been developed by the Earth System Research Laboratory at NOAA to serve users needing short-range weather forecasts [*Benjamin et al.*, 2004]. RUC runs operationally at the National Centers for Environmental Prediction (NCEP). The reanalysis version of RUC data has a horizontal resolution (20 km), 50 vertical computational levels typically from surface to 45–60 hPa), and state of the art analysis and model physical parameterizations [*Benjamin et al.*, 2004]. Hourly analysis data of air temperature at 2 m height (TMP), surface relative humidity (RH), wind speed at 10 m (WS), and height of planetary boundary layer (HPBL) at a 20×20 km^2 spatial resolution are used in this study. Intercomparison studies of RUC analysis with METAR provides a RMS difference of 1.5 m s^{-1} and >1.5 K in wind speed and temperature, respectively, and varies as a function of the season [*Benjamin et al.*, 2004]. HPBL is one of the important parameters in evaluating air quality from satellite data. It is a diagnostic variable in the RUC reanalysis and it is calculated using vertical profiles of virtual potential temperature. To our knowledge validation of RUC HPBL is not available. However, we use this as a surrogate for aerosol height since routine measurements are not available over the entire area of study.

4. Development of Multiple Regression Equations

[11] Integrating satellite, surface and meteorological parameters derived from models at the same temporal and spatial scales is one of the important steps toward development and analysis of a statistical model. The integration of these different variables is performed in two steps. First, satellite data are obtained for each PM2.5 ground location, and second RUC20 data are obtained for each satellite PM2.5 data match-up. In our previous study [*Gupta and Christopher*, 2008], we have shown that averaging MODIS AOT over a box size of $0.5° \times 0.5°$ ($\sim 5 \times 5$ pixels) centered around PM2.5 station is appropriate for this type of

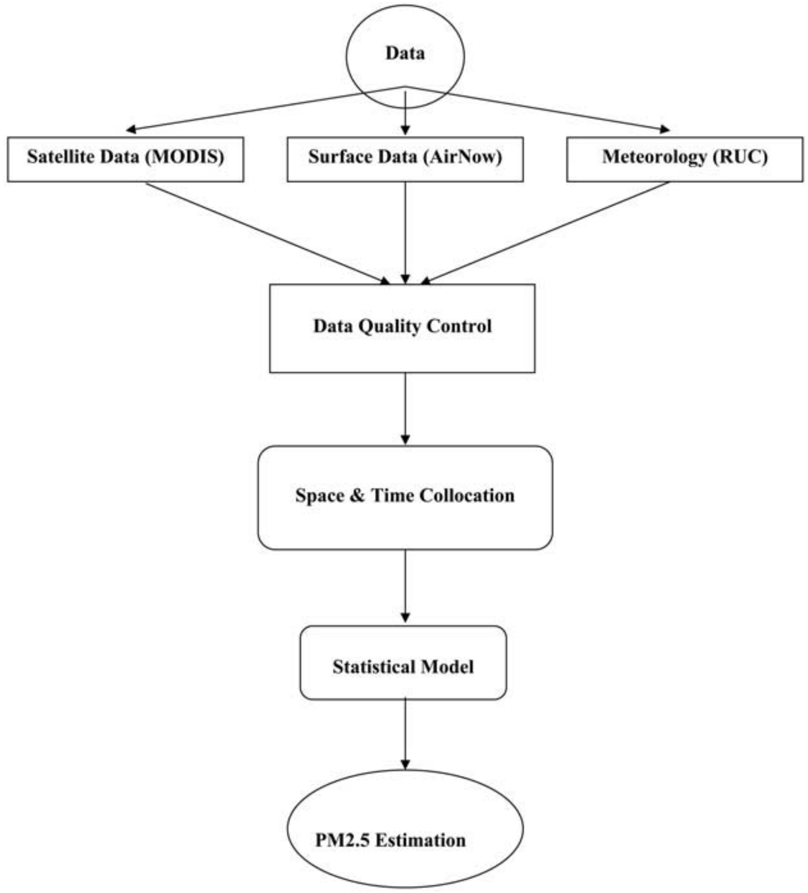

Figure 3. Schematic showing different data sets and framework of model to integrate different data sets for particulate matter air quality.

analysis. We follow the same methodology outlined by *Gupta and Christopher* [2008] to obtain MODIS and RUC parameters over each PM2.5 station. Further screening of the data is done by eliminating all those AOT-PM2.5 pairs where the number of pixels is <3 and the standard deviation in AOT is >0.5. This standard deviation is set to avoid possible cloud contamination in AOT data [*Wang and Christopher*, 2003]. We use hourly measurements of PM2.5, matched with the MODIS Terra AOT closest to the satellite overpass time. The meteorological parameters are also obtained for each AOT-PM2.5 data point by using same spatial and temporal matching approach. The matched data set contains spatiotemporally collocated satellite-derived AOT, cloud fraction (CF), number of pixels (MPIX) used to average AOT values around the PM2.5 station, surface measured PM2.5 mass concentration (PM2.5), and RUC20-derived meteorological fields for 85 P.M2.5 monitoring stations in EPA region 4. The final data set contains 32,834 collocated samples, which are used in development, testing, and validation of the statistical model. To produce the final data set (Satellite Surface Model (SSM) now onward), almost 1TB of combined RUC, MODIS and PM2.5 data has been processed.

[12] Figure 3 provides a flowchart of the methods. First, we developed a simple two-variate method (TVM) equation (equation 1), where MODIS AOT is used to estimate surface level PM2.5 mass concentration. Then, meteorological parameters are added to the analysis to form multiple linear regression (MVM) equations (equation 2) to estimate PM2.5 mass concentration.

[13] Regression coefficients were calculated using SSM data sets for equations (1) and (2) and then these equations are used to calculate PM2.5 mass concentration using input parameters from satellite and RUC meteorological fields. The general form of TVM model is shown in equation (1) and the MVM model in equation (2):

$$PM2.5 = C + M * AOT \tag{1}$$

$$\begin{aligned} PM2.5 = C_1 + C_2 * AOT + C_3 * TMP + C_4 * RH + C_5 * HPBL \\ + C_6 * WS + C_7 * CF \end{aligned} \tag{2}$$

where PM2.5 is PM2.5 mass concentration (μgm^{-3}), AOT is MODIS AOT at 0.55 μm (unit less), C is the intercept and M is slope for the TVM. The Y intercept represents values of PM2.5 when satellite-derived AOT is zero. In other words it represents satellite detection limit of PM2.5. The slope represents PM2.5 mass concentration per unit AOT assuming intercept is zero. C_1 is intercept for the MVM whereas C_2–C_7 are regression coefficients for predictor variables including AOT, temperature (K), relative humidity (%), height of planetary boundary layer (m), wind speed (m s^{-1}), and cloud fraction (%), respectively.

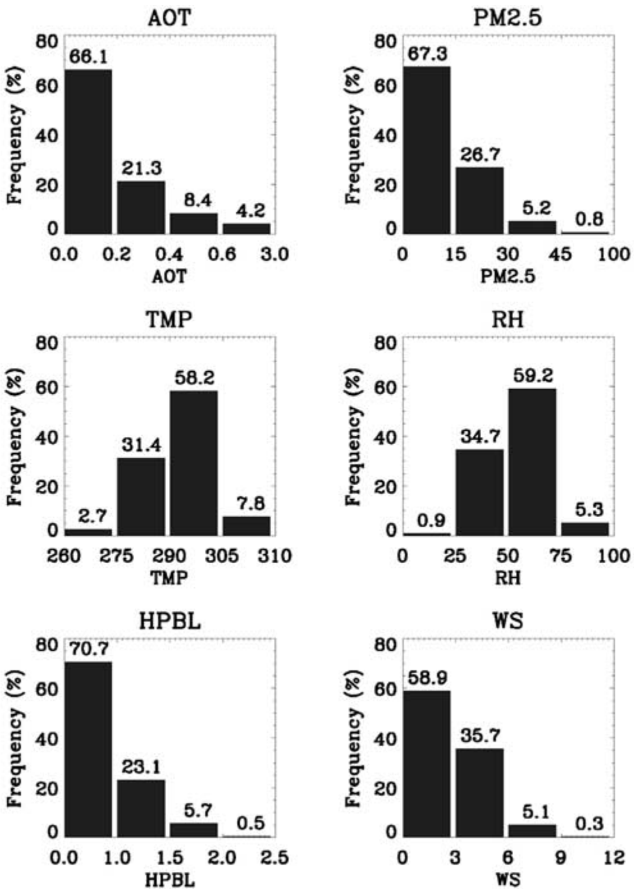

Figure 4. Frequency distribution of all the relevant variables used in assessment of particulate matter air quality. AOT is from MODIS satellite; PM2.5 is from ground measurements; and TMP, RH, HPBL, and WS are from RUC reanalysis.

[14] To obtain an overview of the parameters used in these two methods, the frequency distribution of all variables is shown in Figure 4. The frequency distribution of AOT and PM2.5 are similar, indicating that AOT and PM2.5 are indeed related to each other. All of the variables show significant seasonal variability. The mean MODIS AOT value is 0.19 and the corresponding PM2.5 mass concentration has a mean value of 13.5 μgm^{-3}. AOT values during summer are the highest (0.35 ± 0.22) with low values (0.08 ± 0.09) during the winter. Summer values are typically higher owing to several possible reasons, including enhanced production of secondary particles and enhanced scattering efficiencies of hygroscopic particles. Summer mean AOT values are 40–50% higher when compared to mean AOT values in spring (0.18 ± 0.16) and fall (0.14 ± 0.15). Similar seasonal variations are also seen in PM2.5 mass concentration with largest mean value (20.3 ± 10.5 μgm^{-3}) observed in summer and lowest mean (8.6 ± 6.2 μgm^{-3}) in winter season. Similar to AOT values, the mean PM2.5 mass concentration in fall (13.4 ± 9.4 μgm^{-3}) and spring (11.6 ± 7.2 μgm^{-3}) seasons is almost the same.

[15] Recently, USEPA has made the standards more stringent and has revised the 24-h PM2.5 National Ambient Air Quality Standard (NAAQS) from 65 μgm^{-3} to 35 μgm^{-3} while annual average standard remains the same at 15 μgm^{-3} [*Environmental Protection Agency*, 2006]. The range of PM2.5 mass shows (Figure 4) that air quality over these stations reached moderate to unhealthy categories at certain times, but their frequencies are much lower (30% for moderate and 2% for unhealthy) when compared to good (68%) air quality conditions. The HPBL have the highest values during summer with mean values of 0.94 ± 0.5 km, which is about 50% higher than HPBL values in winter (0.46 ± 0.29 km). Higher values of HPBL in summer can be expected because of higher solar heating during summer seasons [*Stull*, 1988]. Relative humidity varies between 47% and 60% for different seasons with highest in summer and lowest in winter. Since the TEOM measures the $PM_{2.5}$ mass under RH conditions between 40 and 50%, the $PM_{2.5}$ values represent dry aerosol mass, and under dry conditions (RH < 50%) MODIS AOT is more representative of $PM_{2.5}$ mass concentration.

5. Results and Discussions

[16] The results and discussions are organized as follows. Section 5.1 discusses and compares the performance of the two methods (TVM and MVM). Section 5.2 discusses the seasonal differences in the methods. Section 5.3 describes results from MVMs derived for every 2° × 2° subregion to assess the AOT-PM2.5 relationships due to changes in geographical location. In section 5.4, the impact of meteorological parameters on these relationships is analyzed.

5.1. Performance of Two-Variate and Multivariate Methods

[17] We first evaluate the MVM by comparing it with the two-variate AOT-PM2.5 method. The linear correlation coefficients (R) and slopes (M) of the regression lines between estimated and observed PM2.5 mass is calculated for each PM2.5 location. Confidence level of multiple regression equations have been assessed by using *F* tests for each station. Our results are significant with 99% confidence level (α = 0.01), The p value for all of stations was <0.0001 except at station number 14, 20, and 46 where number of data points were sufficiently low (<25). Figure 5 (top) shows the change in R value for each station (*x* axis). Red and blue lines show the absolute values of R for the TVM and MVM, respectively, whereas the green line shows the percentage improvement in R value while using MVM when compared to the TVM. The R values between the estimated and observed PM2.5 using the TVM varies from 0.18 to 0.81 with a mean value of 0.60. Positive values of fractional improvement in R (green) clearly shows that the inclusion of meteorology in the analysis improved the estimation of PM2.5 mass concentration over each station. The improvement in R value varies for each location and ranges from 5% to almost a threefold increase with an average improvement of 21%. The stepwise regression analysis shows that there is a 7% increase in correlation coefficient when surface temperature (TMP) is added to the TVM. This improvement has been observed for all other variables as they are added in a stepwise manner to the analysis (Table 2). This 21% improvement in correlation coefficient reduced the error (percentage error of estimation) by 13% and 17% in estimating hourly and daily average

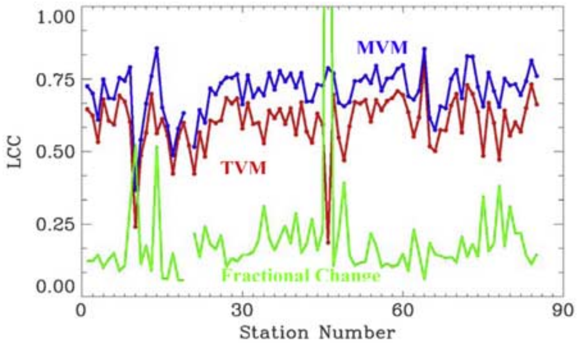

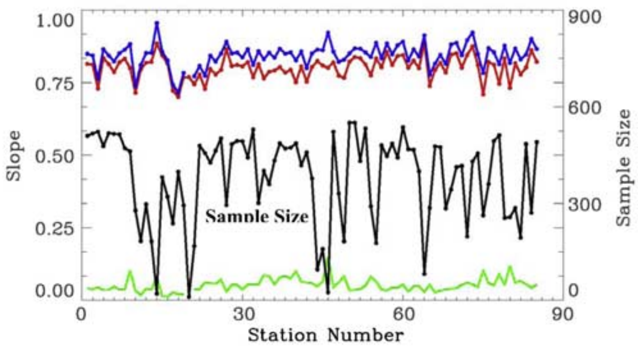

Figure 5. Variations in linear correlation coefficient and slope as function of stations for two-variate (red) and multivariate (blue) models. Also plotted are the number of data points used in the regression equation on secondary *y* axis (black line). The green line shows fractional improvement in linear correlation coefficient and slope in top and bottom, respectively.

PM2.5 mass concentrations, respectively. Incrementally adding other variables in a stepwise manner such as RH, WS, and other parameters only provided slight improvements in correlation coefficients (Table 2).

[18] While the satellite remote sensing community is interested in improving the satellite retrieved AOD to the surface-measured PM2.5 by using meteorological variables, it is equally interesting to see if the use of meteorological parameters alone can help assess PM2.5. Therefore in Table 2 we show the results of PM2.5 estimations by using only the meteorological fields. Table 2 is generated using all the hourly data sets together and this analysis is not performed separately over each station. To accomplish this, AOT has been removed from the model number 6 (Table 2) and PM2.5 mass concentrations have been estimated. Interestingly, the meteorology-only regression model produced almost similar correlation coefficients (0.58) between observed and estimated PM2.5 to those obtained using AOT alone (0.60). However, there are some variations in the values of R from station to station.

[19] This analysis implies that RUC meteorology alone or MODIS AOT alone can be used to estimate PM2.5 with similar uncertainty but, combining the meteorology and MODIS AOT together improves the estimation accuracies by about 13% and 17% for hourly and daily mean PM2.5 values. Also, satellite-derived AOTs are routinely available on a global basis and can be used to assess pollution transport and air quality, especially in regions where ground monitors are unavailable. Coupled with meteorology, satellite-derived AOT appears to be a powerful tool for assessing ground level PM2.5 air quality.

[20] The MVM estimates PM2.5 mass using satellite and meteorological field with an average error of 34% and 24% for hourly and daily PM2.5 averages. There is some variation in this error estimate over different areas as well as with seasons. Improved estimation of PM2.5 from satellite observations can serve as a tool to monitor air quality in the areas where surface monitoring stations are not available. Also, further improvement and modification to current MVM can serve as a valuable air quality assessment tool in such areas. The MVM linear correlation value ranges from 0.37 to 0.86 with mean value of 0.71. Some locations have very limited sample size (<100) as shown in Figure 5 (bottom). There are many possible reasons for low sampling, which includes persistent cloud cover, no aerosol retrieval due to surface conditions, and lack of PM2.5 measurements. These stations (14, 20, 44, 46, and 64) are shown in Figure 2. Owing to the very small (25) sample size over station number 46 (MS), the improvements in correlation should be interpreted with caution. Similarly, station numbers 14 and 20 also have low sample sizes.

[21] Figure 5 (bottom) shows the slope of the linear relationship between observed (*x* axis) and estimated (*y* axis) PM2.5 using the TVM and MVM and the corresponding improvements. All slope values have been calculated by forcing intercept to zero. Slope values have also increased for MVM and the improvement ranges from 1% to 15% with mean value of 5%. The small ranges of slope (0.7 to 0.88 for TVM, and 0.72 to 0.95 for MVM) shows the stable nature of PM2.5-AOT relationships from station to station. However, analysis of the actual data over every single station shows a significant reduction in the scatter between estimated and observed PM2.5 mass when meteorology is included in the analysis. A slope value close to 1 indicates that the estimated and observed PM2.5 mass concentrations are very close to each other. Slope values obtained from MVM has definitely improved the estimation and has also reduced the error in deriving air quality index. This would improve the accuracy of health alerts being issued to the

Table 2. Linear Correlation Coefficient, Slope, and Intercept for Different Multivariate Models to Estimate PM2.5 Mass Concentration as a Function of Different Independent Variables

Model	Independent Variable	R	Change in R (%)	Slope	Intercept
1	AOT	0.604	-	0.37	*8.6*
2	AOT, TMP	0.648	7.3	0.42	*7.8*
3	AOT, TMP, RH	0.662	9.6	0.43	*7.6*
4	AOT, TMP, RH, HPBL	0.670	10.9	0.45	*7.3*
5	AOT, TMP, RH, HPBL, WS	0.677	12.1	0.45	*7.2*
6	AOT, TMP, RH, HPBL, WS, CF	0.683	13.1	0.46	*7.1*

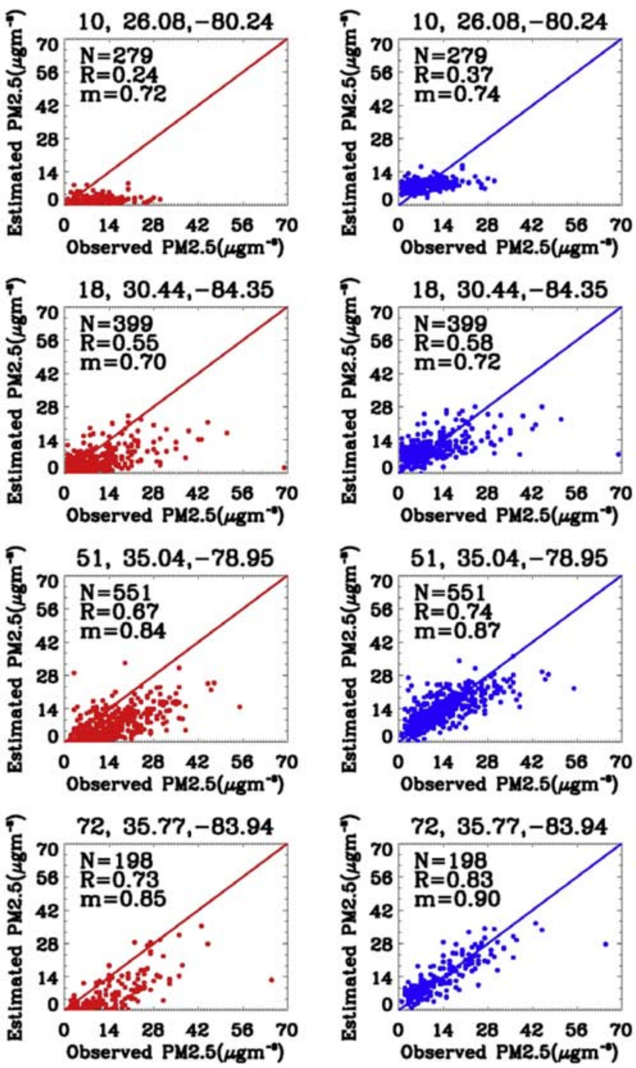

Figure 6. Scatterplot for two-variate and multivariate model estimated PM2.5 and observed PM2.5 for selected stations. (left) Results from the two-variate model; (right) Results from the multivariate model. Station number and latitude/longitudes are given on top of each plot.

public where monitors are absent, being quite beneficial to the society.

[22] Figure 6 shows some selected examples of the scatterplots between observed and estimated PM2.5 mass using the two methods (Figure 2, highlighted as green dots). These sites were selected to show the variability of performance of the method over different locations. Figure 6 (left, red color symbol) shows the scatterplot between observed and estimated PM2.5 mass using TVM, whereas Figure 6 (right, blue colored symbol) is from the MVM. The bottom two plots (2 stations) show the cases where significant improvement in estimation is achieved while using MVM whereas the top two plots (2 stations) shows similar amount of improvement, but not sufficient and estimations are still poor. Further analysis shows that both the stations (top two, 10 and 18) are located close to the coastal region, where uncertainty in the MODIS retrieval could be high [*Remer et al.*, 2005] and the improvement in estimation is due to inclusion of meteorology. Stepwise multiple regression analysis over these four stations (Figure 6) reveals that different meteorological parameters are responsible for the improvement over each site. The first-order improvement at station 10 is mainly due to inclusion of HPBL, whereas second-order improvement is due to inclusion of MODIS cloud fraction (CF). However, note that this is a coastal site and the original relationship between AOT and PM2.5 is not strong due to uncertainties associated with satellite AOT retrievals that contain mixed land-ocean surface reflectance. Similar analysis at station number 18 shows that HPBL, CF, and WS equally contributed to the observed slight (0.03) improvement. However, Figure 6 (station number 18) clearly shows that underestimation in the TVM at lower range of PM2.5 has improved significantly owing to inclusion of meteorological parameters. A first-order improvement at station number 51 and 72 (bottom two plots in the Figure 6) is mainly due to inclusion of temperature whereas all other model variables contributed almost equally. Root-mean-square error (RMSE) values are reduced by 46% (10 to 5.4 μgm^{-3}) and 40% (9.5 to 5.6 μgm^{-3}) for station number 72 and 51, respectively, when the MVM model is used over the TVM model. On the other hand, station number 10 and 18 present only about 20% reduction in RMSE values.

[23] In all the cases, the estimated PM2.5 mass is underestimated by both the methods especially for high (PM2.5 > 45 μgm^{-3}) PM2.5 mass concentrations. Slope values of <1.0 confirm this underestimation over all stations. There could be many possible causes for the underestimation. It is possible for multiple layers of aerosols to be present in the atmosphere and these aerosols are contributing more toward total aerosol optical thickness then surface level aerosols and hence under such conditions AOT-PM2.5 might not be well correlated. In most of the cases, the high concentration of PM2.5 mass could be associated to specific pollution event or transport of the pollution from different source regions. There is also overestimation in PM2.5 for lower range of PM2.5 values.

5.2. Seasonal Analysis

[24] The seasonal analysis is focused on understanding the differences in model slopes and correlation coefficients as well as the change in performance of the two methods over each season. Seasons are defined as spring (March–May), summer (June–August), fall (September–November) and winter (December–February). Figure 7 presents the scatterplots between observed and estimated PM2.5 mass concentration using MVM model for each season. Each plot also shows the correlation coefficient ($R_{2,}$ in red) derived using TVM model. The sample sizes for March–May (8878), September–November (8426), June–August (7874), and December–February (7278) are approximately the same. Slope values are less than one for all four seasons thereby leading to an overall underestimation in PM2.5 mass by both the methods. The mean normalized bias error (MNBE) for lower range (<15 μgm^{-3}) of PM2.5 mass concentration is negative whereas it is positive for upper range of PM2.5 (>45 μgm^{-3}) for all four seasons. The MNBE value is highest in magnitude for winter and summer for lower and upper range of PM2.5, respectively. Again this underestimation in PM2.5 could be due to low

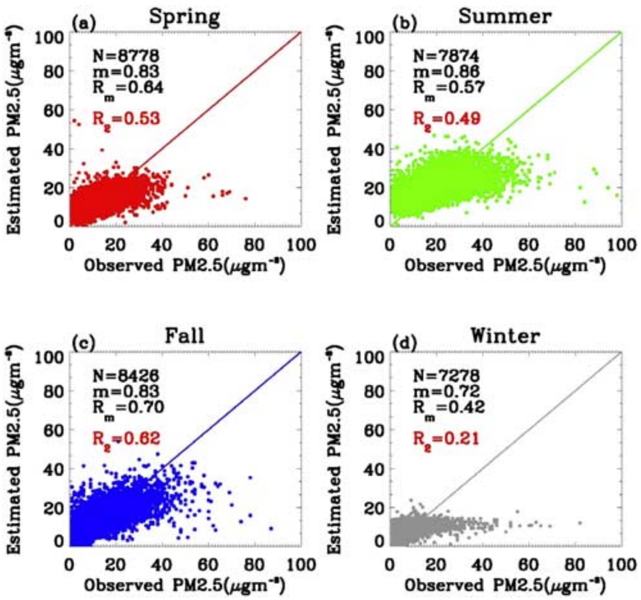

Figure 7. Four seasonal scatterplots showing observed and estimated PM2.5 using multivariate regression model as function of seasons.

number (<1%) of samples of high PM2.5 (>45 μgm^{-3}) values in the analysis. Overestimation in lower range of PM2.5 could be associated with higher uncertainty in AOT retrievals during low aerosol loadings. In the case of low sampling, the current input parameters do not sufficiently represent the relationship between PM2.5 and independent variables. Other meteorological parameters such as vertical temperature gradient, emission factors, removal processes may also be responsible, which controls the particle concentration at the surface and have not been included in current analysis and are probably more suitable for a numerical modeling analysis. Accurate estimation of PM2.5 from these methods require accurate input parameters and any uncertainty in input variables will propagate to the output and will have affects on estimated air quality index. The estimations are the best during spring and fall seasons that have the highest number of data points. Both methods perform better during summer whereas they are very poor in winter season, although MVM shows improvement in correlation from 0.21 to 0.42 compared to TVM during winter. Percentage change in error of estimation is highest during fall (13%) and spring (13%) whereas it is least in summer (6%) with moderate (10%) in winter season. In all four cases, high values of PM2.5 mass concentration (>45 μgm^{-3}) were underestimated by the model compared to low values of PM2.5. Similar results for high pollution loading were also reported by *Liu et al.* [2005] while using MISR-derived AOT values for PM2.5 estimations.

[25] The poor performance during the winter season is largely due to low AOT values (<0.1), which are associated with high uncertainties (~65%) [*Remer et al.*, 2005]. This conclusion is drawn on the basis of very low correlation values in TVM model results as shown R_2 in Figures 7a–7d. Similar results were observed in a study over Sydney, Australia where AOT values were less than 0.1 [*Gupta et al.*, 2007]. Including meteorology in the analysis (i.e., MVM model) improves the results. Again HPBLs are observed to be lower in winter by almost 50% than during the summer season. Lower HPBLs in the winter season that do not allow mixing of pollution in longer air column plays an important role in underestimation of PM2.5 during this season. Section 5.2 discusses more details on the impact of meteorology, which varies between seasons that leads to seasonal differences in estimation of PM2.5 mass.

5.3. Geographical Differences

[26] Geographical differences in model coefficients are analyzed by assessing the methods for every $2° \times 2°$ longitude bin over the southeastern United States. Data from all the stations falling in each grid are grouped and the TVM and MVM as function of seasons are developed. Figure 8 shows scatterplots between observed and estimated PM2.5 mass using MVM models for every grid box. The numbers shown in red inside each scatterplot shows the R values for the TVM model and are used to compare the results from MVM model. The grid between 31 and 33°N and 90–92°W did not have any data during winter and spring season over the entire 3-year time period. A comparison with Figure 2 shows that this grid box contains only one station (42), which has limited number of observations (39 in the summer and 43 in the fall). Again the seasonal pattern over each grid shows almost similar pattern with small variations as seen earlier. The number of available data points and model performance varies with their geographical locations. Correlation coefficients shows good improvement for each box and the degree of improvement varies as a function of location and season. Table 3 summarizes minimum, maximum, mean and standard deviation of improvements in correlation and percentage error of estimation for all the data and for each season. Maximum improvement in mean absolute percentage error of estimation (APE) is observed during fall (19%) and winter (18%) whereas it is 15% and 11% during spring and summer months.

5.4. Model Performance Under Different Meteorological Conditions

[27] Model performance under different meteorological conditions is evaluated by analyzing the model results as function of each meteorological parameter. These include HPBL, TMP and RH. Figures 9, 10, and 11 show the performance of the MVM as a function of HPBL, RH, and TMP, respectively. Each plot in Figures 9–11 also shows the number of data points (N), linear regression line (Y = mX), linear correlation coefficients (R_m: for MVM and R_2: for TVM). Multivariate models are developed for four different ranges of HPBL: surface to 1km, 1 to 1.5 km, 1.5 to 2.0 km, and 2 to 2.5 km (Figure 9). Note the number of available data points in each bins reduced drastically for higher HPBL values, which shows that region of study does not experience frequent high mixing layer during the satellite (Terra) overpass time. Linear correlation coefficient values derived for TVM (R_2) in each HPBL bin shows significant improvement under high HPBL conditions and varies between 0.57 and 0.73 for low to high HPBL bins. Similarly, correlation values for MVM model also shows improvement for all HPBL bins. The correlation improve-

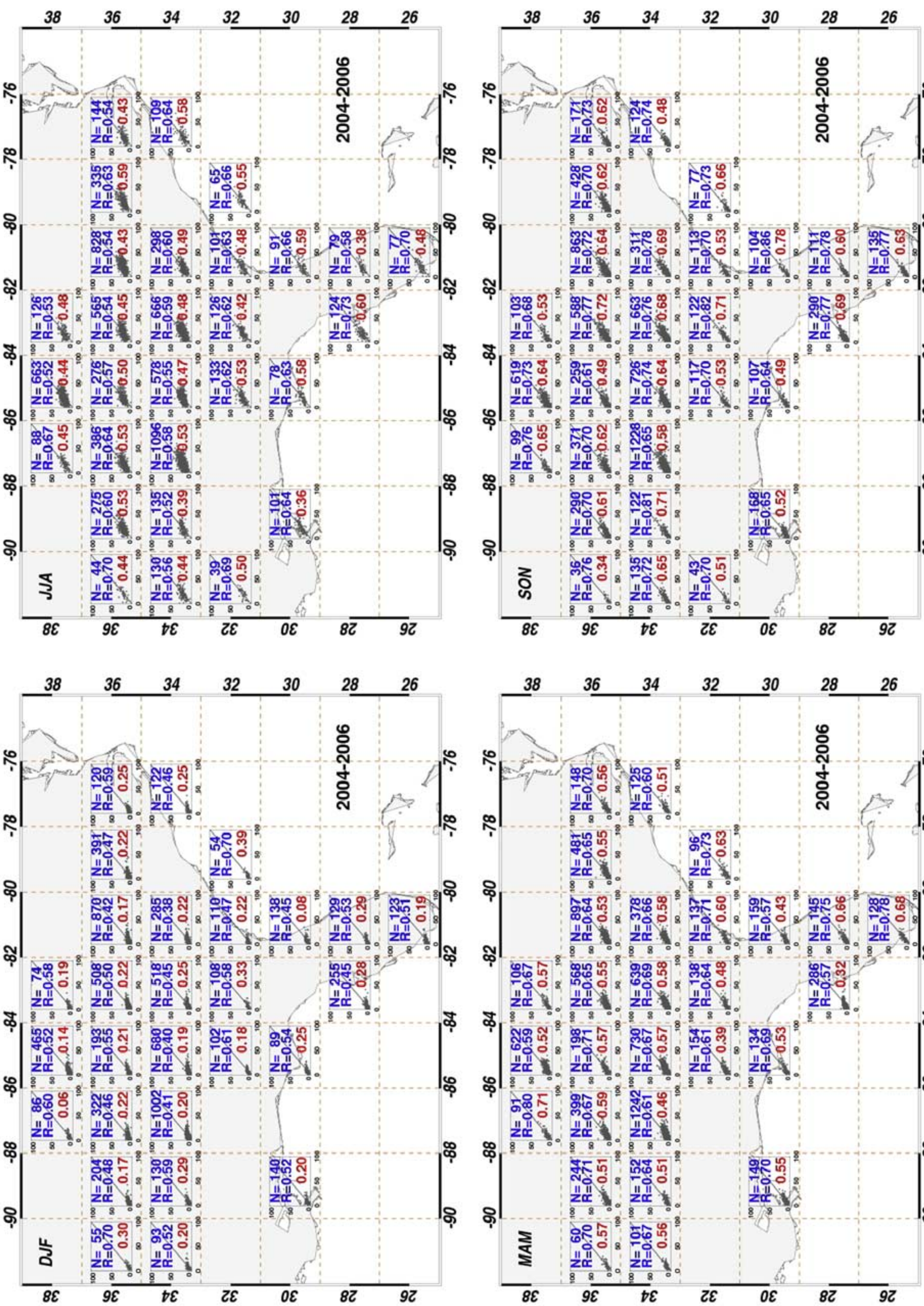

Figure 8. Seasonal map showing scatterplot between estimated and observed PM2.5 in each two by two degree grid box using multivariate models. Also presented is linear correlation coefficient value (red) for the two-variate model.

Table 3. Summary of Statistics From Geographical Two-Variate and Multivariate Model Performance as a Function of Seasons[a]

Parameter	TVM-APE (%)	MVM-APE (%)	APE-IMP (%)	TVM-R	MVM-R	R-IMP (%)
			Winter			
Minimum	42	32	5	0.06	0.38	37
Maximum	54	48	42	0.39	0.70	91
Mean	49	41	18	0.21	0.51	57
Standard Deviation	3	5	10	0.08	0.09	14
			Spring			
Minimum	33	27	8	0.32	0.57	11
Maximum	44	37	24	0.71	0.80	43
Mean	38	33	15	0.55	0.67	19
Standard Deviation	2	2	3	0.08	0.06	7
			Summer			
Minimum	30	25	1	0.36	0.52	7
Maximum	39	39	38	0.60	0.73	44
Mean	33	30	11	0.49	0.61	20
Standard Deviation	2	3	8	0.06	0.06	10
			Fall			
Minimum	36	28	11	0.34	0.61	7
Maximum	47	38	45	0.78	0.86	55
Mean	41	35	19	0.61	0.73	17
Standard Deviation	3	3	7	0.09	0.06	10

[a]Absolute percentage error (APE) and correlation coefficient (R) are presented for two-variate and multivariate models and percentage improvements. TVM, two-variate model; MVM, multivariate model; IMP, improvement.

ment of 0.09, 0.08, 0.05, and 0.07 for HPBL heights of surface to 1km, 1 to 1.5 km, 1.5 to 2.0 km, and 2 to 2.5 km, respectively. Correlation is highest (0.8) between estimated and observed PM2.5 values for HPBL > 2 km. The higher correlation for higher HPBL clearly shows that under a well-mixed boundary layer, satellite measurements (and hence retrievals) of aerosols represents surface level PM2.5 more accurately.

[28] Figure 10 presents the scatterplots between observed and estimated PM2.5 mass using MVM for four different bins of RH. The model performance is best for RH range of 25% to 50%, which is also close to PM2.5 measurement condition (40%) in TEOM. Also, it is important to note that under all ranges of humidity conditions; the estimation of PM2.5 is improved using MVM when compared to the TVM. Similarly, Figure 11 shows the impact of surface temperature on model performance. TMP also impacts the model performance, but it is relatively small and variations in model parameters are less for different range of TMP. High temperature conditions can enhance the emission of

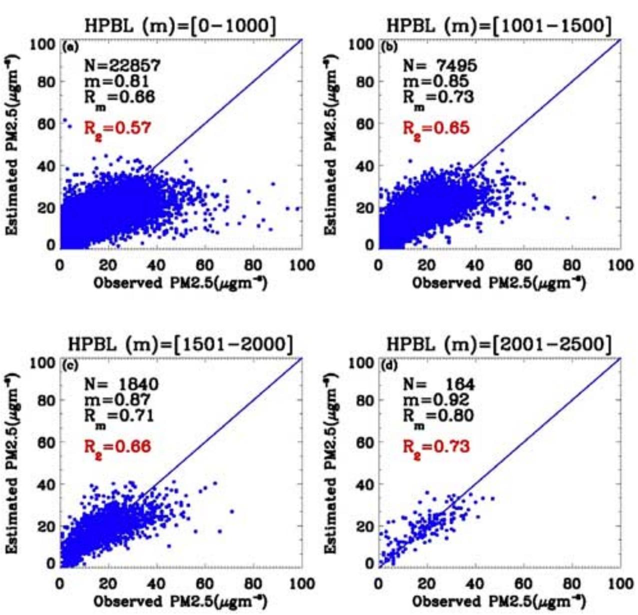

Figure 9. Scatterplot between observed and estimated PM2.5 mass concentration using the multivariate model for four different bins of height of planetary boundary layer.

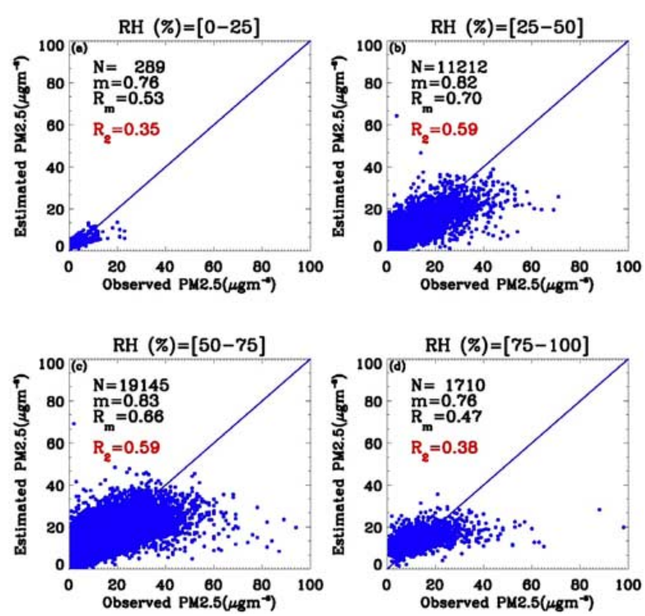

Figure 10. Scatterplot between observed and estimated PM2.5 mass concentration using the multivariate model for four different bins of relative humidity.

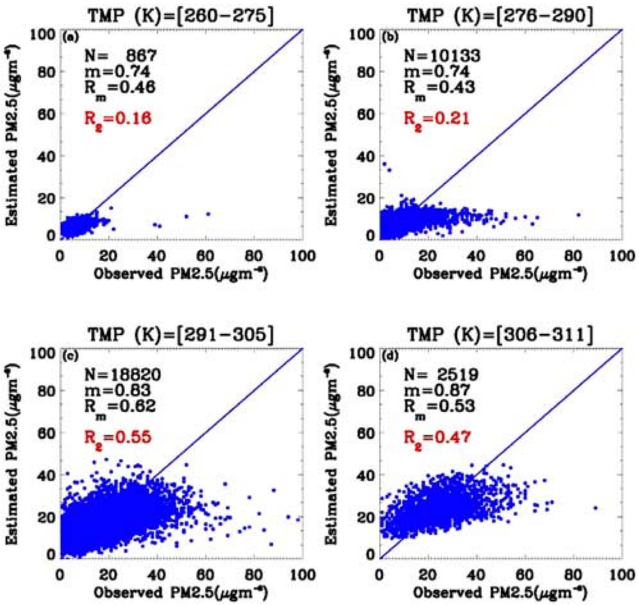

Figure 11. Scatterplot between observed and estimated PM2.5 mass concentration using the multivariate model for four different bins of surface temperature.

particles from surface as well as accelerate the formation of secondary particles in the atmosphere.

6. Summary and Conclusions

[29] Satellite remote sensing is an emerging and promising tool for monitoring aerosol pollution at global scales with high temporal and spatial resolution [*Al-Saadi et al.*, 2005]. This is especially attractive in regions or countries where ground measurements are not available or not possible where remote sensing owing to its reliable repeated coverage can serve as a cost effective tool. However, satellites provide columnar measurements and ancillary pieces of information are required to convert this columnar measurement to surface values. A commonly used method is to form linear relationships between columnar satellite-derived AOT and surface PM2.5 from ground monitors and to extend these relationships to other regions where ground monitors are not available. Aerosol observations from both geostationary and polar orbiting satellites have been used successfully to assess this method. In this study, we take this analysis a step further to determine if meteorological fields can help improve this AOT-PM2.5 relationship.

[30] Therefore, aerosol measurements from MODIS-Terra, meteorological parameters from RUC20, and PM2.5 mass concentrations from surface stations over entire southeastern United States for a 3-year time period have been analyzed for assessing surface level PM2.5. Multivariate statistical models have been developed as function of regions and season to estimate surface level PM2.5 mass concentration while making use of satellite and model data sets. Our results indicate that these models provide improved estimations of PM2.5 mass concentration over two variable regression equations used in previous studies [*Wang and Christopher*, 2003; *Engel-Cox et al.*, 2004]. Linear correlation coefficients between observed and estimated PM2.5 mass concentration show an average improvement of 21% over different stations (99% significance) in the region while using the MVM model over TVM model. Improvements are seen during spring and fall compared to summer season while the results during winter are still very poor although about 18% improvement is seen in error of estimation. The seasonal differences in performance of model are mainly associated with satellite data quality, type and level of pollution and the highly variable nature of local meteorological conditions which plays an important role in formation and removal of PM2.5 in the earth atmosphere. Geographical differences in accuracies of estimated PM2.5 mass are observed when models were developed for each $2^\circ \times 2^\circ$ region. The significant conclusions from this study are as follows:

[31] 1. The MVM provides improved estimations of surface PM2.5 mass concentration when compared to TVM and it is a function of location and season.

[32] 2. Stepwise multiple regression analysis shows that the first-order influence on PM2.5-AOT relationship is temperature when included in the regression and a second-order impact is due to inclusion of boundary layer height, although TMP and HPBL are coupled. This order of importance may also be related with current level of uncertainty involve in the estimation of HPBL data.

[33] 3. The MVM provides improved estimation ($R \geq 0.8$) of PM2.5 mass concentration under high (>2 km) planetary boundary layer conditions due to the well-mixed nature of aerosol layer.

[34] 4. There are definite seasonal differences in model performance. Models perform best during fall (R = 0.70), moderate during spring (R = 0.64) and summer (R = 0.57) and poor during winter (R = 0.42) season.

[35] 5. Overall, both models tend to underestimate PM2.5 mass concentration during heavy pollution (>45) days under all meteorological conditions and overestimate under very low pollution level (<5 μgm^{-3}).

[36] Although the application of satellite observations in monitoring particulate air quality is useful, there are many issues in applying satellite-derived AOT to estimate surface level PM2.5 mass concentration as discussed in the paper. Most researchers in this field agree that AOT alone cannot be used to estimate surface level pollution with good accuracies. Theoretically, surface level PM2.5 is influenced by various meteorological parameters and therefore including information on local meteorology should improve the estimation accuracies. The current study has used a large database from satellite and surface to demonstrate that there is significant reduction in the error (13%) when local meteorology is used in conjunction with satellite data. On the basis of current analysis, well-mixed boundary layer (about 2 km) with high temperature and dry relative humidity (40–50%) conditions should provide optimal estimation of PM2.5. The current approach shows that without using any complex physical and numerical models, simple statistical models can be used to estimate PM2.5 with an average uncertainty of 34% for hourly and 24% for daily mean mass concentrations. In part 2 (P. Gupta and S. A. Christopher, Particulate matter air quality assessment using integrated surface, satellite and meteorological products: Part II: An artificial neural network approach,

submitted to *Journal of Geophysical Research*, 2009) of this series, we extend the use of meteorological fields to estimate PM2.5 mass concentration from satellite remote sensing data in an artificial neural network framework. The inclusion of meteorology in satellite-based projects such as the Infusing satellite data into Environmental Applications (IDEA) could be beneficial for assessing air quality in areas where ground measurements are not available. Tools like IDEA, which uses near-real-time data sets, should be a perfect project to implement model-derived meteorological fields.

[37] **Acknowledgments.** This research is supported by NOAA Air quality projects at UAH (NA06NES4400008 and NA07NES42800005). Pawan Gupta was supported by NASA Headquarters under the Earth and Space Science Fellowship (NESSF) Grant. MODIS data were obtained from the Level 1 and Atmosphere Archive and Distribution System (LAADS) at Goddard Space Flight Center (GSFC). PM2.5 data were obtained from EPA's Air Quality System (AQS). Special thanks to Dick McNider, Ray Hoff, Arastoo Biazar, and Kirk Fuller for their input.

References

Al-Saadi, J., et al. (2005), Improving national air quality forecasts with satellite aerosol observations, *Bull. Am. Meteorol. Soc.*, *86*(9), 1249–1264, doi:10.1175/BAMS-86-9-1249.

Ansmann, A., D. Althausen, U. Wadinger, K. Franke, D. Müller, F. Wagner, and J. Heintzenberg (2000), Vertical profiling of the Indian aerosol plume with six-wavelength lidar during INDOEX: A first case study, *Geophys. Res. Lett.*, *27*(7), 963–966, doi:10.1029/1999GL010902.

Benjamin, S. G., et al. (2004), An hourly assimilation–forecast cycle: The RUC, *Mon. Weather Rev.*, *132*(2), 495–518, doi:10.1175/1520-0493(2004)132<0495:AHACTR>2.0.CO;2.

Engel-Cox, J. A., C. H. Holloman, B. W. Coutant, and R. M. Hoff (2004), Qualitative and quantitative evaluation of MODIS satellite sensor data for regional and urban scale air quality, *Atmos. Environ.*, *38*, 2495–2509, doi:10.1016/j.atmosenv.2004.01.039.

Engel-Cox, J. A., R. M. Hoff, R. Rogers, F. Dimmick, A. C. Rush, J. J. Szykman, J. Al-Saadi, D. A. Chu, and E. R. Zell (2006), Integrating lidar and satellite optical depth with ambient monitoring for 3-dimensional particulate characterization, *Atmos. Environ.*, *40*, 8056–8067, doi:10.1016/j.atmosenv.2006.02.039.

Environmental Protection Agency (2006), National ambient air quality standards for particulate matter: Final rule 40 CFR part 50, *Fed. Regist.*, *71*(10), 61,144–61,233.

Fernald, F. G. (1984), Analysis of atmospheric lidar observations: Some comments, *Appl. Opt.*, *23*, 652–653, doi:10.1364/AO.23.000652.

Grover, B. D., M. Kleinman, N. L. Eatough, D. J. Eatough, P. K. Hopke, R. W. Long, W. E. Wilson, M. B. Meyer, and J. L. Ambs (2005), Measurement of total $PM_{2.5}$ mass (nonvolatile plus semivolatile) with the Filter Dynamic Measurement System tapered element oscillating microbalance monitor, *J. Geophys. Res.*, *110*, D07S03, doi:10.1029/2004JD004995.

Gupta, P., and S. A. Christopher (2008), Seven year particulate matter air quality assessment from surface and satellite measurements, *Atmos. Chem. Phys.*, *8*, 3311–3324.

Gupta, P., S. A. Christopher, J. Wang, R. Gehrig, Y. C. Lee, and N. Kumar (2006), Satellite remote sensing of particulate matter and air quality over global cities, *Atmos. Environ.*, *40*, 5880–5892, doi:10.1016/j.atmosenv.2006.03.016.

Gupta, P., S. A. Christopher, M. A. Box, and G. P. Box (2007), Multi year satellite remote sensing of particulate matter air quality over Sydney, Australia, *Int. J. Remote Sens.*, *28*, 4483–4498, doi:10.1080/01431160701241738.

Hutchison, K. D., S. Smith, and S. Faruqui (2005), Correlating MODIS aerosol optical thickness data with ground-based $PM_{2.5}$ observations across Texas for use in a real-time air quality prediction system, *Atmos. Environ.*, *39*, 7190–7203, doi:10.1016/j.atmosenv.2005.08.036.

Koelemeijer, R., C. Homan, and J. Matthijsen (2006), Comparison of spatial and temporal variations of aerosol optical thickness and particulate matter over Europe, *Atmos. Environ.*, *40*, 5304–5315, doi:10.1016/j.atmosenv.2006.04.044.

Krewski, D., R. T. Burnett, M. S. Goldberg, K. Hoover, J. Siemiatycki, M. Jerrett, A. Abrahamowicz, and W. H. White (2000), Reanalysis of the Harvard six cities study and the American Cancer Society study of particulate air pollution and mortality, A special report of the institute's particle epidemiology reanalysis project, 97 pp., Health Effects Inst., Cambridge, Mass.

Levy, R. C., L. A. Remer, S. Mattoo, E. F. Vermote, and Y. J. Kaufman (2007), Second-generation operational algorithm: Retrieval of aerosol properties over land from inversion of Moderate Resolution Imaging Spectroradiometer spectral reflectance, *J. Geophys. Res.*, *112*, D13211, doi:10.1029/2006JD007811.

Liu, Y., R. J. Park, D. J. Jacob, Q. Li, V. Kilaru, and J. A. Sarnat (2004), Mapping annual mean ground-level $PM_{2.5}$ concentrations using Multi-angle Imaging Spectroradiometer aerosol optical thickness over the contiguous United States, *J. Geophys. Res.*, *109*, D22206, doi:10.1029/2004JD005025.

Liu, Y., J. A. Sarnat, V. Kilaru, D. J. Jacob, and P. Koutrakis (2005), Estimating ground level PM2.5 in the eastern united states using satellite remote sensing, *Environ. Sci. Technol.*, *39*(9), 3269–3278, doi:10.1021/es049352m.

Melnikov, V. M., D. S. Zrnic, R. M. Rabin, and P. Zhang (2008), Radar polarimetric signatures of fire plumes in Oklahoma, *Geophys. Res. Lett.*, *35*, L14815, doi:10.1029/2008GL034311.

Paciorek, C. J., Y. Liu, H. M. Macias, and S. Kondragunta (2008), Spatio-temporal associations between GOES aerosol optical depth retrievals and ground-level PM2.5, *Environ. Sci. Technol.*, *42*(15), 5800–5806, doi:10.1021/es703181j.

Remer, L. A., et al. (2005), The MODIS aerosol algorithm, products, and validation, *J. Atmos. Sci.*, *62*, 947–973, doi:10.1175/JAS3385.1.

Remer, L. A., et al. (2008), Global aerosol climatology from the MODIS satellite sensors, *J. Geophys. Res.*, *113*, D14S07, doi:10.1029/2007JD009661.

Samet, J. M., M. D. F. Dominici, F. C. Curriero, I. Coursac, and S. L. Zeger (2000), Fine particulate air pollution and mortality in 20 U.S. Cities, 1987–1994, *New. Engl. J. Medicine*, *343*(24), 1742–1749, doi:10.1056/NEJM200012143432401.

Seinfeld, J. H., and S. N. Pandis (2006), *Atmospheric Chemistry and Physics: From Air Pollution to Climate Change*, John Wiley, Hoboken, N. J.

Stull, R. B. (1988), *An Introduction to Boundary Layer Meteorology*, *Atmos. Oceanogr. Sci. Libr. Ser.*, vol. 13, 670 pp., Kluwer Acad., Dordrecht, Netherlands.

van Donkelaar, A., R. V. Martin, and R. J. Park (2006), Estimating ground-level $PM_{2.5}$ using aerosol optical depth determined from satellite remote sensing, *J. Geophys. Res.*, *111*, D21201, doi:10.1029/2005JD006996.

Wang, J., and S. A. Christopher (2003), Intercomparison between satellite-derived aerosol optical thickness and $PM_{2.5}$ mass: Implications for air quality studies, *Geophys. Res. Lett.*, *30*(21), 2095, doi:10.1029/2003GL018174.

Wang, J., and S. T. Martin (2007), Satellite characterization of urban aerosols: Importance of including hygroscopicity and mixing state in the retrieval algorithms, *J. Geophys. Res.*, *112*, D17203, doi:10.1029/2006JD008078.

Winker, D. M., J. R. Pelon, and M. P. McCormick (2003), The CALIPSO mission: Spaceborne lidar for observation of aerosols and clouds, *Proc. SPIE Int. Soc. Opt. Eng.*, *4893*, 1–11, doi:10.1117/12.466539.

S. A. Christopher and P. Gupta, Department of Atmospheric Sciences, University of Alabama in Huntsville, Huntsville, AL 35806, USA.